Kuang-Han Chu, Young Soo Joung, Ryan Enright, Cullen R. Buie, and Evelyn N. Wang

Additional information on Appl. Phys. Lett.

Hierarchically structured surfaces for boiling critical heat flux enhancement

Kuang-Han Chu,[1] Young Soo Joung,[1] Ryan Enright,[2,a)] Cullen R. Buie,[1] and Evelyn N. Wang[1,b)]

[1]*Department of Mechanical Engineering, Massachusetts Institute of Technology, 77 Massachusetts Avenue, Cambridge, Massachusetts 02139, USA*

[2]*Thermal Management Research Group, Efficient Energy Transfer (ηET) Dept., Bell Labs Ireland, Alcatel-Lucent, Blanchardstown Business & Technology Park, Snugborough Rd., Dublin 15, Ireland*

We report large enhancements in critical heat flux (CHF) on hierarchically structured surfaces, fabricated using electrophoretic deposition of silica nanoparticles on microstructured silicon and electroplated copper microstructures covered with copper oxide (CuO) nanostructures. A critical heat flux of $\approx 250 \, \text{W/cm}^2$ was achieved on a CuO hierarchical surface with a roughness factor of 13.3, and good agreement between the model proposed in our recent study and the current data was found. These results highlight the important role of roughness using structures at multiple length scales for CHF enhancement. This high heat removal capability promises an opportunity for high flux thermal management. © 2013 AIP Publishing LLC [http://dx.doi.org/10.1063/1.4801811]

The large latent heat associated with the liquid-vapor phase transition makes two-phase cooling a promising approach to address challenges in high heat flux thermal management applications.[1–4] In a boiling heat transfer system, the critical heat flux (CHF), where a vapor film will begin to cover the heated surface leading to a loss of contact between the surface and the liquid, represents the operational limit due to the significant reduction in heat transfer coefficient. Therefore, methods to extend CHF have been studied extensively owing to its significant practical importance in high performance thermal management systems.[5–11] Our recent study utilized well-defined silicon micropillar arrays to demonstrate the role of increasing surface roughness factor (i.e., $r =$ total surface area/projected surface area) for CHF enhancement on complete wetting surfaces, where the apparent contact angle is $\beta = 0°$.[12] The developed CHF model, based on roughness-amplified capillary forces pinning the contact line of vapor bubbles, showed good agreement with experimental data for microstructured surfaces with $1 \leq r \leq 6$, with even higher CHF values predicted with increasing r. In this work, we fabricated both silica and copper oxide (CuO)-based hierarchical surfaces with $r \approx$ 3.6–13.3 to further increase CHF and support the concept that introducing hierarchy produces a multiplicative effect on contact line pinning forces. Accordingly, we demonstrated $q_c'' \approx 250 \, \text{W/cm}^2$ with a wall superheat of $\approx 33 \, \text{K}$ on the roughest sample tested, representing a $\approx 200\%$ increase in CHF compared to smooth SiO_2 reference surfaces. The obtained CHF values on the hierarchical surfaces showed good agreement with the model prediction, which supports our physical view of the enhancement phenomenon and the multiplicative effect of roughness at distinct length scales. This predictable high heat removal capability using scalable fabrication techniques promises an exciting opportunity for new surface designs for high flux thermal management.

In our recent study, the CHF condition was predicted based on a force balance between the evaporating vapor momentum, buoyancy, and surface forces acting on the liquid/vapor interface of an individual bubble.[7] Our proposed model, however, decoupled the bubble geometry from the surface force. Accordingly, the surface force maintaining the position of the contact line is amplified due to a longer effective contact line length on the structured surfaces, leading to an expression in the following form:[12]

$$q_c'' = K \times h_{fg} \rho_g^{1/2} [\sigma_{lv} g (\rho_l - \rho_g)]^{1/4}, \qquad (1)$$

where

$$K = \left(\frac{1 + \cos \beta}{16} \right) \left[\frac{2(1 + \alpha)}{\pi (1 + \cos \beta)} + \frac{\pi}{4} (1 + \cos \beta) \cos \psi \right]^{1/2},$$

$\alpha = r \cos \theta_{rec}$ is the amplified surface force term, θ_{rec} is the liquid receding angle on the corresponding smooth surface (i.e., intrinsic receding angle), σ_{lv} is the liquid-vapor surface tension, and ψ is the inclination angle of the surface (i.e., $\psi = 0$ for a horizontal upward facing surface). In the super-hydrophilic wetting regime ($\beta = 0°$), Eq. (1) shows a proportional increase in CHF with the parameter K, which, in turn, is proportional to the square root of the roughness factor r through α, i.e., $q_c'' \propto \sqrt{r}$. Therefore, further enhancement in CHF should increase monotonically with increasing roughness factor. Indeed, we demonstrated that experimental pool boiling data on microstructured surfaces with roughness factors r ranging from 1.8 to 6 followed this scaling, with reasonable quantitative agreement despite several simplifying assumptions used in the model development.[12]

To achieve higher roughness factors, $r > 6$, we used two fabrication methods to realize hierarchical surfaces with two distinct length scales.[13] Silica-based, superhydrophilic, hierarchical surfaces were fabricated by microstructuring silicon via deep reactive ion etching (DRIE) followed by the

---

a)Work initiated while affiliated with Department of Mechanical Engineering, Massachusetts Institute of Technology, 77 Massachusetts Avenue, Cambridge, Massachusetts 02139, USA and Stokes Institute, University of Limerick, Limerick, Ireland.

b)Author to whom correspondence should be addressed. Electronic mail: enwang@mit.edu
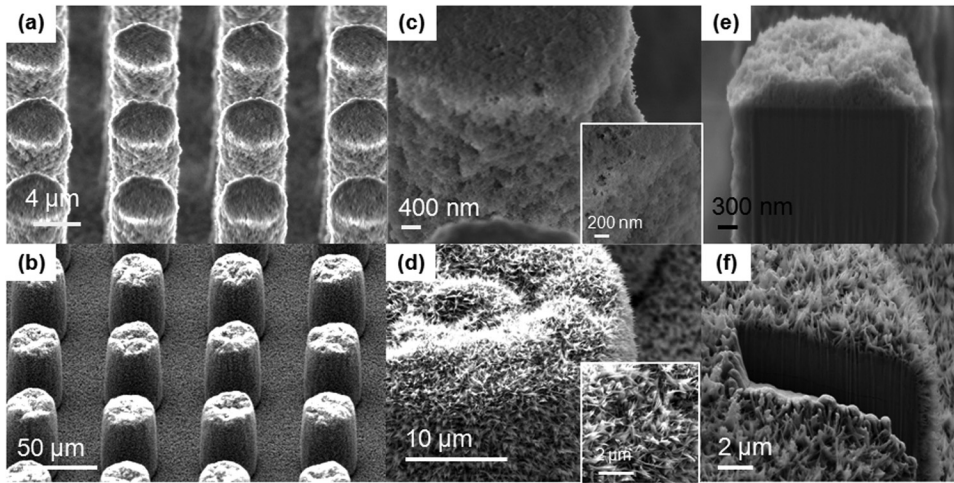
FIG. 1. SEMs of the representative, fabricated silica- and CuO-based hierarchical surfaces. (a) EPD-coated silica, micropillars in a square array with heights of $10\,\mu m$, diameters of $10\,\mu m$, and spacings of $5\,\mu m$, and (b) CuO micropillars in a square array with heights of $61\,\mu m$, diameters of $30\,\mu m$, and spacings of $30\,\mu m$. (c) Magnified view of the silica-based micropillar and EPD-coated SiO_2 nanoparticles (inset). (d) Magnified view of the CuO micropillar and CuO nanostructures formed on the surfaces (inset). (e) Cross-section view of the silica-based micropillar and (f) cross-section view of the CuO micropillar obtained using FIB milling.

electrophoretic deposition (EPD) of $14\,nm$ diameter SiO_2 nanoparticles.[13] Details of the EPD process can be found in previous work.[14] This square array of Si microstructures had heights of $10\,\mu m$, diameters ranging from $5-10\,\mu m$, and spacings of $5-15\,\mu m$. CuO-based, superhydrophilic hierarchical surfaces were fabricated by electroplating Cu micropillars followed by a chemical oxidation step to form CuO nanostructures.[13,15] The electroplated square array of Cu micropillars had heights ranging from $35-68\,\mu m$, diameters of $30-35\,\mu m$, and spacings of $30\,\mu m$. Scanning electron micrographs (SEMs) representative of the realized hierarchical surfaces are shown in Figs. 1(a)–1(d). Also, shown in Figs. 1(e) and 1(f) are the cross-section images of the hierarchical structures obtained using focused ion beam (FIB) milling. Finally, on all surfaces, a $1\,\mu m$ thick layer of Cu was deposited on the back side of the silicon substrates to facilitate solder attachment of the samples to the test setup. Upon dicing, the samples had a projected surface area of $2 \times 2\,cm^2$, which is large enough to be considered representative of an infinite plate for water[16,17] and is of comparable size to typical high heat flux electronic components. The heat transfer performance of the hierarchical surfaces was measured using an experimental pool boiling setup.[12] All tests were performed using degassed, high purity water (Chromasolv for HPLC, Sigma-Aldrich) to avoid premature bubble formation and minimize surface contamination.

To estimate the surface roughness factors r of the EPD-coated silica surfaces, we characterized the roughness factors of the nanoscale structure component, r_n, using atomic force microscopy (AFM) and cross-section images by FIB[13] milling. For the CuO surfaces, however, r_n was difficult to measure by AFM due to the high aspect ratio of the CuO nanostructures and characteristic length of the spacing between the nanostructures, and by cross-section imaging due to deposited byproduct of ablation on the surface during FIB milling process.[13] Accordingly, the results using AFM, FIB images, and contact angle measurement may not reflect the condition that the vapor bubble is in contact with the surfaces (i.e., true contact line length).[13] Therefore, we extracted the r_n of the CuO nanostructures from CHF data obtained on a nanostructured CuO surface using our CHF model (Eq. (1)). The effective r_n on our CuO nanostructured surfaces estimated by this indirect approach was ≈ 4.8. We note that the CuO nanostructures on both the smooth and the

microstructured Cu surfaces were formed using the same oxidation conditions. The total roughness factors, r, were then calculated as the product of r_n and roughness factor of the micropillars r_m (i.e., $r = r_n \times r_m$). Both hierarchical surface types demonstrated superhydrophilic behavior at room temperature due to the large roughness factors obtained, $r > 6$, and the high surface energy of SiO_2 and CuO.

Figure 2 shows the heat flux q'' as a function of wall superheat $\Delta T = T_w - T_{sat}$, where T_w is the heated surface temperature and T_{sat} is the saturation temperature (i.e., boiling curve) for the Si-silica- and Cu-CuO-based hierarchical surfaces. Reference boiling curves obtained for smooth SiO_2 surfaces ($r \approx 1$) are also shown in Fig. 2 for comparison. Details of the tested surface geometries are listed in Table I. The maximum uncertainty of the heat flux and temperature measurements was calculated to be $\approx 5.6\%$ and $\pm 1.8\,K$, respectively.[13] While a CHF of $\approx 83\,W/cm^2$ was obtained on the smooth SiO_2 (Sm) surfaces, CHF values of $236\,W/cm^2$ and $250\,W/cm^2$ were demonstrated on the best performing Si-silica (EPD-Hier3) and Cu-CuO-based (CuO-Hier3)
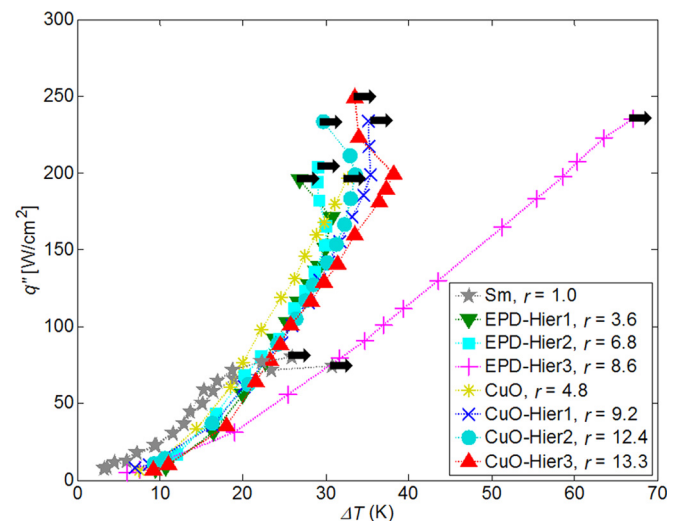

FIG. 2. Boiling curves on the smooth ($r = 1$) and structured ($r > 1$) surfaces detailed in Table I. The arrows indicate the CHF condition. The consistency and accuracy of the measurements are demonstrated by the two nearly identical boiling curves for the smooth surface. The boiling curves show a clear trend of increasing CHF with surface roughness due to roughness-augmented capillary forces.

TABLE I Geometric parameters of the hierarchical surfaces. The units of height, diameter and (center-to-center) spacing for micropillars, and thickness of nanostructures are in microns (μm). The roughness factor of the microstructure, r_m, is calculated with $r_m = 1 + \pi dh/(d+s)^2$. The effective roughness factor of the contact line, r, is the product of the roughness factors at the micro and nanoscales, i.e., $r = r_m \times r_n$.

Sample no.	Height (h)	Diameter (d)	Spacing (s)	Thickness (t)	r_m	r_n	r
Sm	n/a	n/a	n/a	n/a	1.0	1.0	1.0
EPD-Hier1	20	10	15	0.15	2.01	1.9	3.8
EPD-Hier2	20	10	5	0.15	3.79	1.9	7.2
EPD-Hier3	20	5	10	0.45	2.40	3.7	8.9
CuO	n/a	n/a	n/a	1	1.0	4.8[a]	4.8
CuO-Hier1	35	30	30	1	1.91	4.8[a]	9.2
CuO-Hier2	61	30	30	1	2.59	4.8[a]	12.4
CuO-Hier3	68	35	30	1	2.78	4.8[a]	13.3

[a]Estimation based on the CHF model and experimental CHF values on CuO nanostructured surfaces.

FIG. 3. CHF as a function of $\alpha \, (= r \cos \theta_{rec})$. The proposed model (solid line) is compared to the K-Z with a factor of $K = 0.18$ (dashed line). The symbols show the CHF data for (●) microstructured surfaces (see Ref. 8), and (▲) EPD-coated SiO$_2$ and (▼) CuO hierarchical surfaces, as a function of the estimated α values.

hierarchical surfaces, respectively. The significant enhancement in CHF on the hierarchical surfaces (up to 200%) is attributed to the high surface roughness factor, which provides a large surface force to balance the momentum force due to evaporation.[12] In addition, the sudden reduction in superheat ΔT along the boiling curve of hierarchical surfaces (i.e., "kickback") is indicative of nucleation sites within the nanostructures becoming active.[18] The high roughness factor of the nanostructure on sample EPD-Hier3 was a result of the thick deposited silica layer (450 nm) due to a longer EPD deposition time (30 s).[13] However, the resulting thermal resistance due to the thick silica layer on sample EPD-Hier3 was estimated to be at least $\approx 3\times$ higher than the nanostructure coatings on the other samples (EPD-Hier1-2, CuO, and CuO-Hier1).[13] While similar characteristics were evident in all of the other hierarchical surface boiling curves, the boiling curve of the sample EPD-Hier3 demonstrated a low slope and a high superheat ($\Delta T \approx 68 \pm 3.8\,^{\circ}C$) at CHF due to the high thermal resistance of the thick EPD coating, leading to a low heat transfer coefficient.[13]

In Fig. 3, the predicted CHF as a function of α (Eq. (1)) is overlaid with data from our experiments for the hierarchical surfaces (in red) and previously tested microstructured surfaces[12] (in blue). The dashed line represents the CHF predicted by the classical Kutateladze-Zuber (K-Z) model[19,20] (hydrodynamic instability mechanism) using an empirical factor of $K = 0.18$ in Eq. (1)[21] obtained from classical pool boiling experiments on unstructured, well-wetting surfaces ($\alpha \approx 1$). The good agreement between the data and the model, which does not contain any fitting parameters, for α ranging from 1 to ≈ 13.3 demonstrates the validity of the model for the structured surfaces in the complete wetting regime. The trend of increasing CHF with increasing surface roughness is well-captured by the model which suggests that the key physics of the CHF mechanism on these structured surfaces was accounted for. While the value of r_n of the CuO surfaces was approximated based on the CHF model and experimental data of CuO nanostructured surfaces, the agreement between the CHF on CuO hierarchical surfaces (CuO-Hier1-CuO-Hier3) and the model prediction was consistent, suggesting
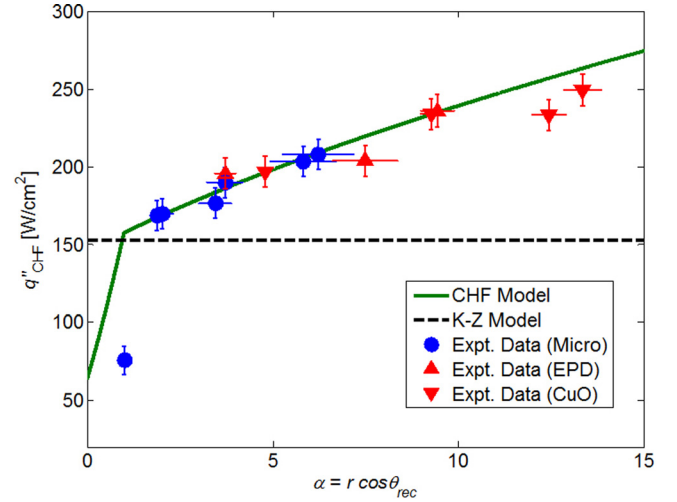
that the effective surface roughness pinning the vapor bubble based on the indirect approach for our CuO nanostructured surfaces provided a reasonable estimation.

In conclusion, we fabricated hierarchically structured surfaces using electrophoretic deposition on microstructured silicon, and electroplated and oxidized copper with a roughness factor, r of ≈ 3.6–13.3, to investigate the CHF condition on high roughness factor surfaces in pool boiling. The good agreement between the CHF model and the experimental observations on the hierarchical surfaces indicates that the roughness-amplified surface force plays the defining role in CHF enhancement on structured surfaces with a roughness factor r ranging from 1 to 13.3 where distinct roughness length scales introduce a multiplicative effect on the amplified surface force. A CHF of 250 W/cm^2, a $\approx 200\%$ CHF enhancement compared to smooth SiO$_2$ surfaces, achieved on CuO-based hierarchical surfaces demonstrates high heat removal capability. While the thick EPD-coated silica hierarchical surfaces have a high surface roughness factor, the high thermal resistance presents challenges with this approach for practical implementation. CuO hierarchical surfaces, on the other hand, can provide high roughness factors without a significant increase in thermal resistance. This finding highlights the importance of the surface structure thermal characteristics resulting from a particular synthesis technique so that enhanced CHF can be obtained without sacrificing heat transfer performance. Furthermore, the scalable fabrication process of electroplating copper micropillars coupled with a simple chemical oxidation process promises an exciting opportunity to achieve high performance boiling heat transfer.

[1]D. C. Price, IEEE Trans. Compon. Packag. Technol. **26**(1), 26–39 (2003).

[2]T. W. Kenny, K. E. Goodson, J. G. Santiago, E. N. Wang, J.-M. Koo, L. Jiang, E. Pop, S. Sinha, L. Zhang, D. Fogg, S. Yao, R. Flynn, C.-H. Chang, and C. H. Hidrovo, Int. J. High Speed Electron. Syst. **16**(1), 301–313 (2006).

[3]J. R. Thome, Heat Transfer Eng. **27**(9), 1–3 (2006).

[4]E. Pop, Nano Res. **3**, 147–169 (2010).

[5]J. Mitrovic, Int. J. Therm. Sci. **45**, 1–15 (2006).

[6]R. Chen, M.-C. Lu, V. Srinivasan, Z. Wang, H. H. Cho, and A. Majumdar, Nano Lett. **9**(2), 548–553 (2009).

[7]S. G. Kandlikar, J. Heat Transfer **123**, 1071–1079 (2001).

[8]E. Forrest, E. Williamson, J. Buongiorno, L.-W. Huc, M. Rubner, and R. Cohen, Int. J. Heat Mass Transfer **53**, 58–67 (2010).

[9]C. H. Li and G. P. Peterson, Front. Heat Mass Transfer (FHMT) **1**, 023007 (2010).

[10]S. Kim, H. D. Kim, H. Kim, H. S. Ahn, H. Jo, J. Kim, and M. H. Kim, Exp. Therm. Fluid Sci. **34**(4), 487–495 (2010).

[11]H. S. Ahn, H. J. Jo, S. H. Kang, and M. H. Kim, Appl. Phys. Lett. **98**, 071908 (2011).

[12]K.-H. Chu, R. Enright, and E. N. Wang, Appl. Phys. Lett. **100**(24), 241603 (2012).

[13]See supplementary material at http://dx.doi.org/10.1063/1.4801811 for the fabrication processes, surface roughness characterization, thermal resistance calucalation, and experimental setup.

[14]Y. S. Joung and C. R. Buie, Langmuir **27**(7), 4156–4163 (2011).

[15]Y. Nam, S. Sharratt, C. Byon, S. J. Kim, and Y. S. Ju, J. Microelectromech. Syst. **19**(3), 581–588 (2010).

[16]T. G. Theofanous, J. P. Tu, A. T. Dinh, and T. N. Dinh, Exp. Therm. Fluid Sci. **26**(6–7), 775–792 (2002).

[17]M.-C. Lu, R. Chen, V. Srinivasan, V. P. Carey, and A. Majumdar, Int. J. Heat Mass Transfer **54**(25–26), 5359–5367 (2011).

[18]V. P. Carey, *Liquid-Vapor Phase Change Phenomena* (Taylor & Francis, Bristol, 1992).

[19]N. Zuber, AEC Report No. AECU-4439, 1959.

[20]S. S. Kutateladze, Kotloturbostroenie **3**, 10–12 (1948).

[21]W. M. Rohsenow, J. P. Hartnett, and E. N. Ganic, *Handbook of Heat Transfer Fundamentals*, 2nd ed. (McGraw-Hill, New York, 1985).